Near-zero dispersion, highly nonlinear lead-silicate W-type fiber for applications at 1.55μm

Angela Camerlingo, Xian Feng*, Francesco Poletti, Giorgio M. Ponzo, Francesca Parmigiani, Peter Horak, Marco N. Petrovich, Periklis Petropoulos, Wei H. Loh, and David J. Richardson

Optoelectronics Research Centre, University of Southampton, Southampton, SO17 1BJ, UK
**xif@orc.soton.ac.uk*

Abstract: We report the design, fabrication and characterization of a lead-silicate glass highly nonlinear W-type fiber with a flattened and near-zero dispersion profile in the 1.55 μm region. The fiber was composed of three types of commercial lead silicate glasses. Effectively single-mode guidance was observed in the fiber at 1550nm. The nonlinear coefficient and the propagation loss at this wavelength were measured to be 820 $W^{-1}km^{-1}$ and 2.1dB/m, respectively. Investigations of the Brillouin threshold revealed no evidence of stimulated Brillouin scattering for continuous wave signal powers up to 29dBm in a 2m sample of the fiber. A broadband dispersion measurement confirmed the near-zero dispersion values and the flat dispersion profile around 1550nm, in good agreement with our simulations. Efficient four-wave-mixing, tunable across the whole C-band, was demonstrated in a 2.2m length of the fiber.

OCIS codes: (060.2280) Fiber design and fabrication; (060.4370) Nonlinear optics, fibers

References and links

1. J. Hansryd, P. A. Andrekson, M. Westlund, J. Li, and P. O. Hedekvist, "Fiber-Based Optical Parametric Amplifiers and their Applications," IEEE J. Sel. Top. Quantum Electron. **8**(3), 506–520 (2002).
2. J. Y. Y. Leong, P. Petropoulos, J. H. V. Price, H. Ebendorff-Heidepriem, S. Asimakis, R. Moore, K. Frampton, V. Finazzi, X. Feng, T. M. Monro, and D. J. Richardson, "High nonlinearity dispersion-shifted lead-silicate holey fibers for efficient 1μm pumped supercontinuum generation," J. Lightwave Technol. **24**(1), 183–190 (2006).
3. H. Ebendorff-Heidepriem, P. Petropoulos, S. Asimakis, V. Finazzi, R. C. Moore, K. Frampton, F. Koizumi, D. J. Richardson, and T. M. Monro, "Bismuth glass holey fibers with high nonlinearity," Opt. Express **12**(21), 5082–5087 (2004).
4. X. Feng, T. M. Monro, V. Finazzi, R. C. Moore, K. Frampton, P. Petropoulos, and D. J. Richardson, "Extruded single-mode, high-nonlinearity, tellurite glass holey fibre," Electron. Lett. **41**(15), 835–837 (2005).
5. L. Fu, V. G. Ta'eed, E. C. Magi, I. C. M. Littler, M. D. Pelusi, M. R. E. Lamont, A. Fuerbach, H. C. Nguyen, D. I. Yeom, and B. J. Eggleton, "Highly nonlinear chalcogenide fibres for all-optical signal processing," Opt. Quantum Electron. **39**(12-13), 1115–1131 (2007).
6. S. Fujino, H. Ijiri, F. Shimizu, and K. Morinaga, "Measurement of viscosity of multi-component glasses in the wide range for fibre drawing," J. Jpn. Instrum.Met. **62**, 106–110 (1998).
7. A. Camerlingo, F. Parmigiani, X. Feng, F. Poletti, P. Horak, W. H. Loh, D. J. Richardson, and P. Petropoulos, "Four-wave mixing-based wavelength conversion in a short-Length of a solid 1D microstructured fibre," *ECOC*, Th. 9.1.3,Vienna, (2009).
8. S. Asimakis, P. Petropoulos, F. Poletti, J. Y. Y. Leong, R. C. Moore, K. E. Frampton, X. Feng, W. H. Loh, and D. J. Richardson, "Towards efficient and broadband four-wave-mixing using short-length dispersion tailored lead silicate holey fibers," Opt. Express **15**(2), 596–601 (2007).
9. X. Feng, F. Poletti, A. Camerlingo, F. Parmigiani, P. Horak, P. Petropoulos, W. H. Loh, and D. J. Richardson, "Dispersion-shifted all-solid high index-contrast microstructured optical fiber for nonlinear applications at 1.55 μm," Opt. Express **17**(22), 20249–20255 (2009).
10. Schott E-catalogue, 2000, Optical Glass for Windows, version 1.1E, (Schott Glass, 2001).
11. F. Poletti, V. Finazzi, T. M. Monro, N. G. R. Broderick, V. Tse, and D. J. Richardson, "Inverse design and fabrication tolerances of ultra-flattened dispersion holey fibers," Opt. Express **13**(10), 3728–3736 (2005).
12. A. Camerlingo, F. Parmigiani, X. Feng, F. Poletti, P. Horak, W. H. Loh, D. J. Richardson, and P. Petropoulos, "Wavelength Conversion in a Short Length of a Solid Lead-Silicate Fibre," IEEE Photon. Technol. Lett. **22**(9), 628–630 (2010).

#129039 - $15.00 USD Received 26 May 2010; revised 10 Jun 2010; accepted 10 Jun 2010; published 9 Jul 2010

13. X. Feng, A. K. Mairaj, D. Hewak, and T. M. Monro, "Nonsilica glasses for holey fibers," J. Lightwave Technol. **23**, 62046–62054 (2005).
14. T. Tsumuraya, and M. Suzuki, "Polishing method for inner surface of tubular brittle material and tubular brittle material obtained by polishing method," US Patent No. US 7238089 B2 (Date of Patent: Jul. 3, 2007).
15. A. Boskovic, S. V. Chernikov, J. R. Taylor, L. Gruner-Nielsen, and O. A. Levring, "Direct continuous-wave measurement of n(2) in various types of telecommunication fiber at 1.55 μm," Opt. Lett. **21**(24), 1966–1968 (1996).
16. F. Poletti, K. Furusawa, Z. Yusoff, N. G. R. Broderick, and D. J. Richardson, "Nonlinear tapered holey fibers with high SBS threshold and controlled dispersion," J. Opt. Soc. Am. B **24**(9), 2185–2194 (2007).
17. J. H. Lee, T. Tanemura, K. Kikuchi, T. Nagashima, T. Hasegawa, S. Ohara, and N. Sugimoto, "Experimental comparison of a Kerr nonlinearity figure of merit including the stimulated Brillouin scattering threshold for state-of-the-art nonlinear optical fibers," Opt. Lett. **30**(13), 1698–1700 (2005).
18. H.-T. Shang, "Chromatic dispersion measurement by white-light interferometry on metre-length single-mode optical fibres," Electron. Lett. **17**(17), 603–605 (1981).

1. Introduction

Nonlinear effects in fibers can be exploited for the direct implementation of several key functions, such as wavelength conversion, signal regeneration and the like, which have the potential to radically transform future optical networks. Amongst the various nonlinear effects that can be used in optical processing applications, four-wave-mixing (FWM) is particularly attractive, due to the transparency it offers in terms of bit rate and modulation format. The most important fiber parameters that contribute towards achieving efficient and broadband FWM are a high nonlinear coefficient, low dispersion values over a broad wavelength range, a short fiber length and ideally a high Stimulated Brillouin Scattering (SBS) threshold [1]. To this end, significant research efforts have been devoted to the development of highly nonlinear and dispersion-tailored fibers. High-index soft glasses such as lead silicate, bismuth, tellurite and chalcogenide are well suited to achieving this target and significant progress in fiber fabrication based on these materials has already been attained [2–5]. Amongst these materials, lead silicate represents an attractive family of glasses, as they have higher thermal stability and less steep viscosity curves as compared to other non-silica glass alternatives [6]. On the other hand, high refractive index non-silica glasses are usually characterized by large values of normal dispersion at telecommunication wavelengths [2–5], which can be detrimental for FWM-based applications.

A way to overcome the problem of these high material dispersion values has been offered by the microstructured optical fiber (MOF) technology: the wavelength-scale features of the fiber cladding in MOFs can be designed to provide correspondingly large values of anomalous waveguide dispersion that can be used to tailor the overall fiber dispersion profile. Non-silica glass MOFs therefore combine the great advantage of dramatically increasing the nonlinear coefficient of the fiber, owing to the larger air/glass refractive index contrast and nonlinear refractive index n_2, with the ability to tailor the dispersion profile, by virtue of an engineered cladding structure. Although a great variety of MOFs have been fabricated so far, they can be grouped into two main categories, depending on whether the wavelength-scale features of their claddings consist of an all-solid structure or instead rely on a holey cladding. Both all-solid and holey MOF structures have already been employed in the realization of compact nonlinear systems using non-silica glasses as the fiber materials [7,8]. Although holey structures offer the advantage of being drawn from a single glass, they are prone to structural distortion during the fabrication process, which makes it difficult to control the overall dispersion profile with the required level of accuracy. If two or more compatible glasses with the required refractive index difference are available, however, all-solid MOFs present the clear advantage that the fiber refractive index geometry is defined during preform manufacture and is not prone to additional forms of distortion during the fiber drawing process, making fabrication of the fiber with an accurately defined structure (and hence more uniform and accurately defined dispersive properties) a much easier task. We have previously reported the benefits of an all-solid soft glass MOF over a holey MOF in [9], where we presented a fiber structure with a solid high-index core surrounded by alternating glass rings

#129039 - $15.00 USD Received 26 May 2010; revised 10 Jun 2010; accepted 10 Jun 2010; published 9 Jul 2010

of different refractive indices. This fiber design allowed us to achieve a relatively high nonlinear coefficient of ~120$W^{-1}km^{-1}$ and a reasonably low dispersion value (~12.5ps/nm/km) at 1550nm. In order to enhance the nonlinear coefficient of the fiber we have investigated the possibility of reducing the core size but found that the wavelength-scale features in the microstructured cladding of the fiber then led to an excessive amount of normal waveguide dispersion for small core diameters. This indicated that it is not possible to fabricate such a microstructured fiber having both a high nonlinearity coefficient and a low and flat dispersion profile simultaneously. In the attempt to overcome this problem, we have found that the far simpler W-type structure reported in this work can provide a fiber with a high nonlinear coefficient and a flattened and near-zero dispersion profile within the C-band. In the following sections, we report on the latest results on the fabrication and characterization of this highly nonlinear W-type fiber, which is based on three commercial lead silicate glasses (Schott SF57, LLF1, and SF6). The fiber exhibits a high nonlinear coefficient and low dispersion with a flat dispersion profile at telecommunication wavelengths. Accurate polishing of the constituent elements of the starting glass preform before the fiber drawing has allowed us to achieve a loss value of ~2dB/m, approaching the material loss. The fiber does not show any SBS for values of power as high as 29dBm when using a pure continuous wave (CW) scheme. We also experimentally demonstrate the advantages of using the fabricated dispersion-optimized W-type fiber as the nonlinear medium in a tunable and efficient FWM-based wavelength-conversion scheme using a 2.2m length sample of fiber.

2. Design and fabrication

Optical waveguide theory predicts that for any chosen core material it is always possible to engineer a step-index fiber with a core diameter d_0 and index difference Δn, such that, at a certain wavelength λ_{flat}, the waveguide dispersion exactly compensates for the material dispersion in both *absolute value* and *slope*, thus creating an overall flattened and near-zero dispersion profile around λ_{flat}. Whether in practice a pair of chemically, thermally and mechanically compatible glasses with the required linear refractive indices can be found is, however, a more complex matter. In order to identify two such glasses generating flat dispersion at telecoms wavelengths, we undertook a systematic search within the glass family of lead silicates, which we knew from past experience would possess the required compatibility for fiber drawing. Eventually we discovered that using Schott SF57 (n = 1.80 @ 1530nm) in a d_0~1.65μm core and Schott LLF1 (n = 1.53 @ 1530nm) [10] in the cladding would provide exactly the right amount of waveguide dispersion for an overall flat profile at 1550nm. Figure 1(a) shows the simulated dispersion profile for three different values of core diameter together with the dispersion profile of the bulk SF57. All the simulations in this work have been performed using a full vector Finite Element Method (FEM) solver [11].

#129039 - $15.00 USD Received 26 May 2010; revised 10 Jun 2010; accepted 10 Jun 2010; published 9 Jul 2010

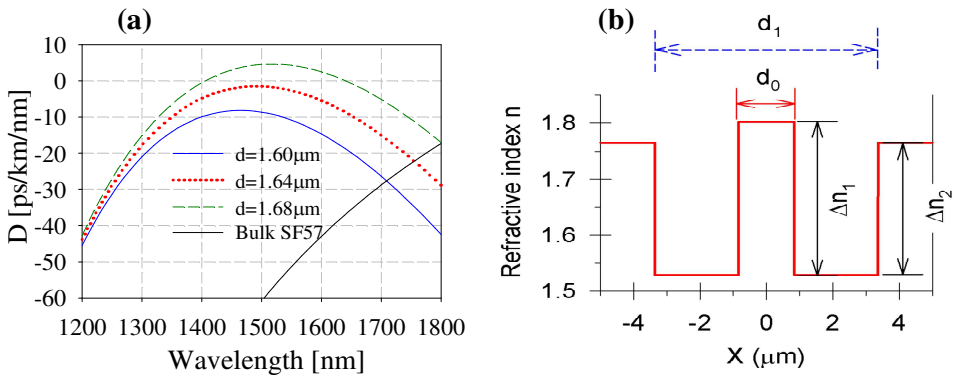

Fig. 1. (a) Numerical simulations of the dispersion profile of the fiber for various core diameters (solid and dashed lines) and dispersion of the bulk glass SF57 (dash-dotted line); (b): Schematic of the W-type index profile of SF57-LLF1-SF6 fiber with high index-contrast.

The large value of normal dispersion exhibited by the bulk SF57 glass at telecom wavelengths can be well compensated for through the waveguide dispersion, thus resulting in a fiber with a low dispersion D (absolute value |D| less than 5ps/nm/km) across the whole wavelength range of 1450nm-1650nm when the core diameter is between 1.64μm and 1.68μm. At these wavelengths, however, the resulting optimized step-index fiber would support a few guided modes. In order to ensure single mode operation we added an additional outer cladding layer with a refractive index higher than the effective index of the high order modes in the core, causing such modes to become extremely lossy. Another Schott glass, SF6 (n = 1.76 @ 1530nm), was identified as the most suitable for this task. By carefully adjusting the inner diameter (ID) of this second cladding to d_1~7.4μm, we could impose a high differential confinement loss between the fundamental and high order core modes, thus ensuring effectively single mode operation in a meter scale device. A schematic of the index profile of the final fiber is shown in Fig. 1(b).

In the first attempt to fabricate this W-type index profiled fiber, the SF57 rod, the LLF1 tube and the SF6 tube were all made by extrusion, as previously reported in [12]. However, this process introduces interface defects, which were identified as the main cause of the relatively high propagation losses observed (~5dB/m) [12]. A fiber fabrication procedure consisting of multiple heating steps often results in higher propagation losses due to the thermally induced refractive index variations within the fiber core. We therefore adopted a room-temperature mechanical process for producing the preform, i.e., based on drill-and-polish approach, to improve the propagation attenuation. As shown in Fig. 2(a), first an LLF1 tube with an outer diameter (OD) of 13.0 (± 0.05) mm and an ID of 3.0 (± 0.05) mm and an SF57 rod with an OD of 2.9 (± 0.05) mm were drilled from the glass bulks using a commercial ultrasonic drilling machine [13]. The outer surface of the rod and both the outer and inner surfaces of the tube were then polished to optical quality to minimize scattering losses due to interface roughness within the final fiber.

The procedure of polishing the surface of the drilled preforms was similar to the procedure introduced in Ref [14]. The outer surface of the tube was polished by means of a rotating hollow tubular polishing head with an ID slightly larger than the target OD of the tube. The inner surface of the hollow polishing head was wound with a diamond abrasive sheet with less than 1μm grain size. During the polishing, the polishing head rotated around the tube, which was firmly held in place, and slowly moved along its axial direction. A similar procedure was employed for polishing the inner surface of the tube, whereby a polishing head with 2.9mm OD was used instead, and the 1μm grain size diamond sheet was attached on the outer surface of the polishing head. The whole procedure took several hours for each preform. After polishing, the surface roughness of the outer surface of the SF57 core rod and the LLF1 tube

#129039 - $15.00 USD Received 26 May 2010; revised 10 Jun 2010; accepted 10 Jun 2010; published 9 Jul 2010

was reduced down to less than 50nm from the initial 5-10μm measured on the drilled rod or tube. A similar reduction in the surface roughness is expected for the inner surface of the LLF1 tube after the polishing. The averaged absolute values of surface roughness Ra, were measured by an Alpha-Step Surface Profiler.

The polished assembly of rod-and-tube was then elongated into a thin cane and subsequently inserted in an extruded SF6 jacket tube. The final W-type fiber was drawn from the resulting rod-in-tube assembly. The scanning electron microscopy (SEM) images of the fiber structure are illustrated in Fig. 2(b). The diameter of the SF57 core and the outer diameter of the LLF1 ring were measured to be 1.63μm and 7.4μm, respectively.

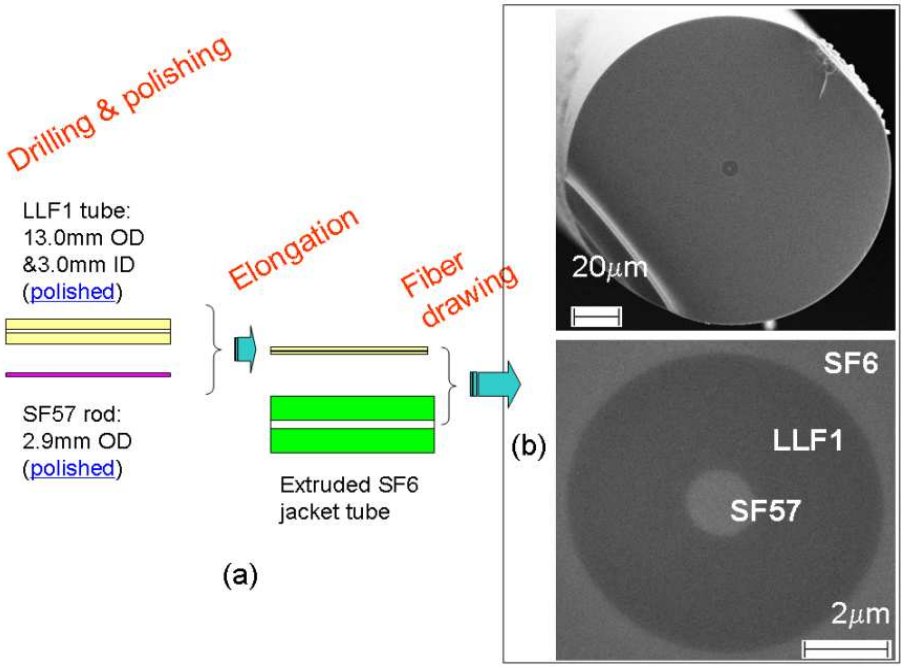

Fig. 2. (a) Schematic of the fabrication of the W-type fiber with improved attenuation; (b) SEM photographs of the fabricated W-type fiber.

3. Modal and nonlinear characterization of the W-type fiber

As described in the previous section, the W-type fiber reported here has been designed to be effectively single mode at 1550nm. Figure 3 shows the corresponding simulated (a) and measured mode (b) at 1550nm, confirming effectively single mode guidance. The accurate polishing procedure employed in the manufacture of the preform resulted in a very substantial reduction of the fiber propagation loss. Using the cut-back technique the propagation loss was measured to be 2.1 ± 0.2dB/m at 1550nm, (see Fig. 3(c)), a significant improvement as compared to the value of 4.8 ± 0.2dB/m measured in the previously reported fiber [12]. Note that the bulk attenuation of commercial Schott SF57 glass is estimated to be 1.5 ± 0.6dB/m at 1.53μm, based on the internal transmittance of glass plates with the thicknesses of 10mm and 25mm [10]. We thus expect to be able to further reduce the overall fiber losses down to the 1dB/m level by careful optimization of the fabrication procedure.

#129039 - $15.00 USD Received 26 May 2010; revised 10 Jun 2010; accepted 10 Jun 2010; published 9 Jul 2010

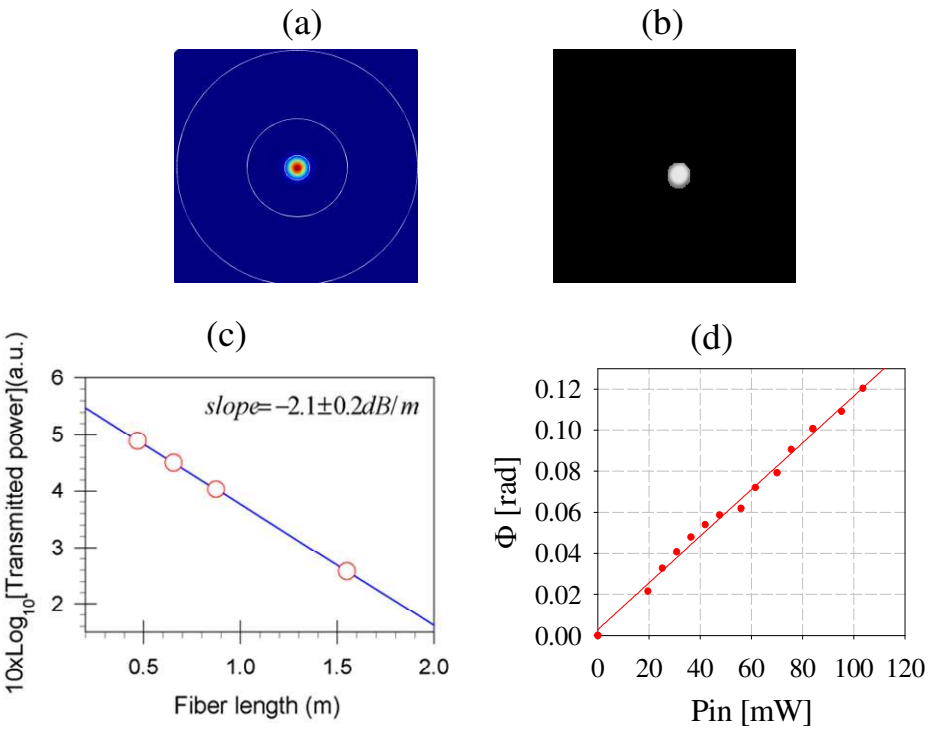

Fig. 3. (a) Simulated and (b) measured LP_{01} mode of the fiber; (c) linear fitting of the transmitted power (on a log scale) from the output end of the fiber, using the cutback method, (d) nonlinear phase shift versus input power measured at the output of the fiber.

The effective nonlinear coefficient of the fiber was measured at 1550nm using the Boskovic method [15]. The nonlinear phase shift measured for the W-type fiber is plotted in Fig. 3(d) as a function of the input power. Taking into account the effective length of the fiber, we estimated the nonlinear coefficient from the linear fit of our measurements to be 820 $W^{1}km^{-1}$. The effective mode area, A_{eff}, of the W-type fiber was numerically calculated from the SEM images of the fiber to be ~1.9μm^2 at 1550nm. From this value and using the value of the nonlinear refractive index, n_2, of the glass used, the nonlinear coefficient of the fiber was calculated to be $830W^{-1}km^{-1}$ at 1550nm, which agrees well with the measured value.

#129039 - $15.00 USD Received 26 May 2010; revised 10 Jun 2010; accepted 10 Jun 2010; published 9 Jul 2010

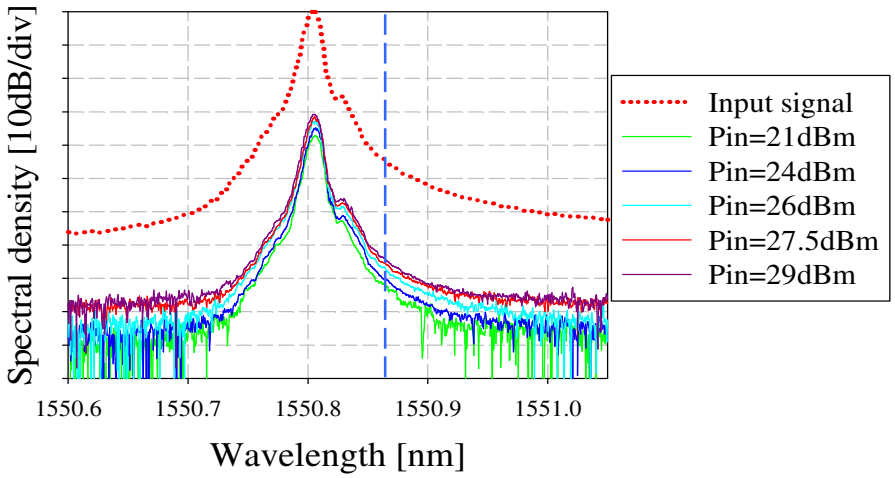

Fig. 4. Spectra of the input (red dotted line) and the output (solid lines) signals reflected back from the W-type fiber for power levels ranging from 20 to 29dBm into the fiber. The vertical dashed line indicates where the SBS shift would be expected. Note that the input signal has been scaled up for visual purposes.

When comparing the properties of highly nonlinear fibers, it often useful to consider their Brillouin gain characteristics alongside the strength of their third-order nonlinearity coefficient. This is especially relevant when considering applications that require a strong CW pump, since the maximum nonlinear phase shift that can occur in the fiber for sources with a bandwidth smaller than the Brillouin linewidth is proportional to the nonlinear coefficient and inversely proportional to the Brillouin gain coefficient. Non-silica glasses typically have a nonlinear refractive index higher than silica by 1-3 orders of magnitude (20 times in the case of SF57), while they show a Brillouin gain that is only a few times larger than that of silica [16]. The Brillouin shift in SF57 has been previously measured to be 7.65GHz [16]. We investigated the Brillouin threshold of this fiber by launching a true CW signal in a 3m long sample and collecting the light reflected back from it and found that no stimulated back-scattered signal could be detected at the expected wavelength for values of power as high as 29dBm in the fiber (the maximum possible launch power in our experiments). In order to place this observation in context we have calculated the SBS power threshold of a common silica highly nonlinear fiber (HNLF) assuming the same HNLF characteristics of the fiber used in [17]. Assuming the same γL_{eff} for the two fibers (the length of the silica HNLF would obviously be much longer than the W-type fiber due to it lower nonlinearity), we estimated an SBS power threshold of just 25dBm for the silica fiber. Similarly, for a simple SF57 based fiber we estimated a 30dBm SBS threshold [16]. Figure 4 shows the input signal (red dotted line) together with the signals reflected back from the fiber (solid lines) for values of input power into the fiber ranging from 20dBm to 29dBm. The blue dashed reference line indicates the wavelength at which the Brillouin reflected signal was expected.

4. Dispersive properties and their role in a FWM-based wavelength converter

The exceptionally low values of chromatic dispersion anticipated in the W-type fiber necessitate the use of a broadband measurement technique for its characterization. We therefore set up a low-coherence Mach-Zehnder interferometric system based on a broadband supercontinuum source (Fianium, SC400) to accurately measure the dispersion profile [18]. Using suitable polarization optics, we obtained two clean interferograms for each of the polarization axes of a 1.27m long sample of the fiber for the wavelength range of 1300nm to 1680nm (for reference, one of the interferograms is shown in Fig. 5(a)). Processing of the data has indicated that the dispersion is minimum at 1525nm (−2.5 ps/nm/km), whereas it is lower

#129039 - $15.00 USD Received 26 May 2010; revised 10 Jun 2010; accepted 10 Jun 2010; published 9 Jul 2010

than −5 ps/nm/km across the whole wavelength range between 1430 and 1600 nm. These values are in good agreement with the simulated dispersion predictions, as illustrated in Fig. 5(b) where the red solid line represents the simulated profile and the blue symbols the measured dispersion values for the fabricated fiber.

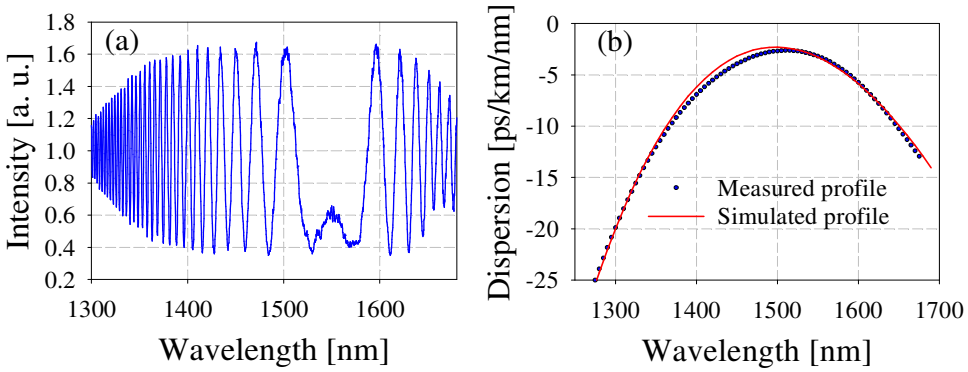

Fig. 5. (a) Observed interferogram of one of the two polarizations propagating in the W-type fiber; (b) Simulated (red solid line) and measured (blue symbols) dispersion curve of the W-type fiber.

In combination, the characteristics of this fiber make it a highly suitable candidate for the realization of compact nonlinear devices based on FWM processes. To demonstrate this point, we implemented a simple FWM-based wavelength conversion scheme in a 2.2m sample of the W-type fiber, as shown in Fig. 6.

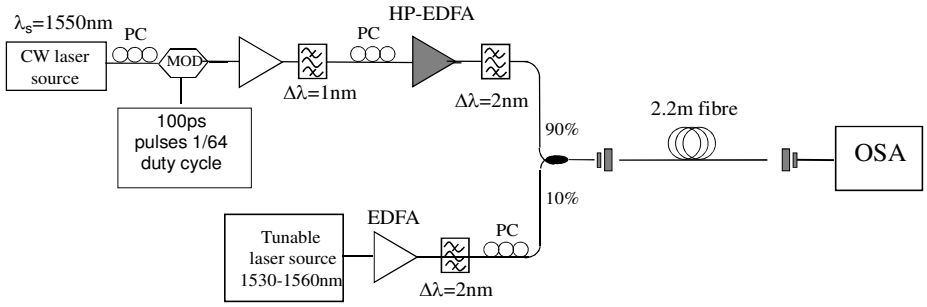

Fig. 6. Experimental setup of FWM-based wavelength conversion scheme.

The pump wave was a CW laser operating at 1550 nm, which was amplitude modulated by a Mach-Zehnder modulator with 100ps rectangular pulses with a duty cycle of 1:64.The modulated signal was amplified and then combined in a 90/10 coupler with an independently amplified CW signal, generated from a tunable laser source. A bandpass filter (BPF) was employed to remove any undesired amplified spontaneous emission (ASE) noise resulting from the EDFA. Polarization controllers (PCs) were used to control the state of polarization of the two beams and to align them to the polarization axis of the fiber. The combined beam was free-space launched into the fiber with a coupling efficiency of ~25%. The average power of the pump and the signal launched into the fiber were 17dBm and 2dBm respectively. Note that the additional components connected to the high power EDFA impose a practical limit on the maximum value of pump power that can be coupled with the signal power. It is also worth noting that as compared to the demonstration presented in [12] the fiber loss reduction to 2.1dB/m (from 4.8dB/m) together with the lower dispersion and dispersion slope values allowed us to employ this simpler quasi-CW pump as opposed to a short-pulse pump used previously.

#129039 - $15.00 USD Received 26 May 2010; revised 10 Jun 2010; accepted 10 Jun 2010; published 9 Jul 2010

We experimented with several signal wavelengths at either side of the pump, ranging from 1530 nm to 1546 nm and 1554 nm to 1570 nm (limited by the range of our tunable source) – see Figs. 7(a) and 7(b). For all of the wavelengths we observed a uniform conversion efficiency of 0 dB, defined as the ratio of the power of the converted idler to the launched signal power. Note that for this calculation an extra 18 dB was added to the (average) values recorded on the optical spectrum analyzer (OSA) to account for the duty cycle of the idlers (as opposed to the CW nature of the signals). Figure 7(c) traces the measured values of conversion efficiency compared to the simulated curves evaluated for the fabricated fiber, exhibiting good agreement between the two, and also providing some information on how the conversion bandwidth is expected to be affected outside this 40-nm range.

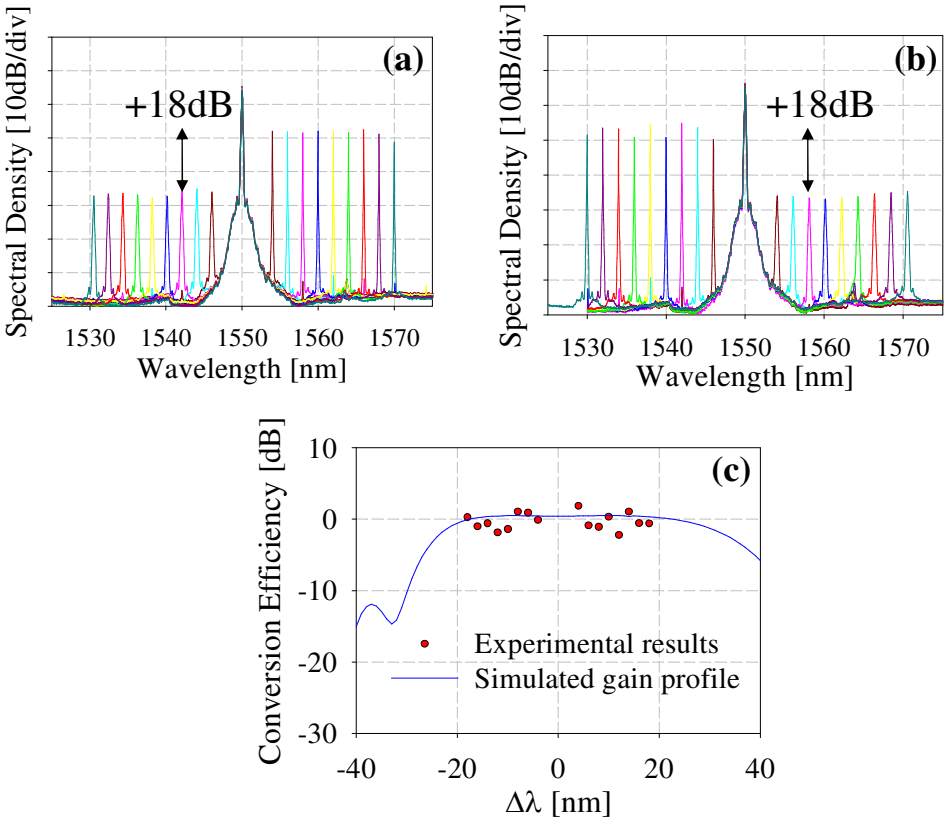

Fig. 7. (a), (b): Measured spectral traces of FWM-based wavelength conversion in a 2.2m-length of W-type fiber using a quasi-CW pump and tunable CW signal; (c) Simulated (solid blue line) and measured (red symbols) curves for the FWM conversion efficiency in the fabricated W-type fiber.

5. Conclusions

We have designed, fabricated and characterized a single mode, highly nonlinear, lead silicate glass based W-type fiber with a flattened and near zero dispersion profile in the 1.55μm region. The nonlinear coefficient and the propagation loss of the fiber at 1550nm have been measured to be $820W^{-1}km^{-1}$ and 2.1dB/m respectively. The dispersion profile has been measured using an interferometric setup and the measurement confirms the predicted ultra-low values of dispersion (normal and between −5 and −2.5ps/nm/km) and dispersion slope (between −0.05 and 0 $ps/nm^2/km$) at telecommunication wavelengths. By rigidly scaling either up or down the fiber dimensions by a few percent it should be possible to obtain

#129039 - $15.00 USD Received 26 May 2010; revised 10 Jun 2010; accepted 10 Jun 2010; published 9 Jul 2010

different values of either anomalous or normal dispersion while maintaining a broadly flat dispersion region in a fiber with similar loss and nonlinearity. We have also investigated the Brillouin threshold of the fiber and observed that no SBS shift could be detected for values of power as high as 29dBm. Finally, we have numerically and experimentally demonstrated the performance of this fiber in a broadband, efficient and broadly tunable FWM-based wavelength conversion scheme. A uniform conversion efficiency of 0 dB was measured across the whole C-band for a peak pump power of 3.1 W.

Acknowledgments

This research has received funding from the Engineering and Physics Science Research Council (UK) and the European Communities Seventh Framework Programme FP/2007-2013 under grant agreement 224547 (PHASORS). Dr F. Poletti gratefully acknowledges the support of a Royal Society University Fellowship.

#129039 - $15.00 USD Received 26 May 2010; revised 10 Jun 2010; accepted 10 Jun 2010; published 9 Jul 2010